

# Optimization on microlattice materials for sound absorption by an integrated transfer matrix method

Xiaobing Cai and Jun Yang<sup>a)</sup>

*Department of Mechanical and Materials Engineering, The University of Western Ontario,  
London, Ontario N6A 5B9, Canada  
caixiaobing11@gmail.com, jyang@eng.uwo.ca*

Gengkai Hu

*School of Aerospace Engineering, Beijing Institute of Technology, Beijing 100081,  
People's Republic of China  
hugeng@bit.edu.cn*

**Abstract:** Materials with well-defined microlattice structures are super-light, stable, and thus bear great potential in sound absorption. An integrated transfer matrix method (TMM) is proposed to evaluate the sound absorbing efficiency of these lattice materials, in which a massive number of micropores are densely placed. A comparison between integrated TMM and conventional TMM reveals that the proposed approach offers better predictions on sound absorption of microlattice. This approach is then employed to optimize the microlattice material to determine the best pore and porosity that lead to maximum absorbing efficiency capability and minimum required thickness to attain a target sound absorption.

© 2015 Acoustical Society of America

[JMD]

**Date Received:** November 6, 2014    **Date Accepted:** March 10, 2015

## 1. Introduction

Materials and structures used for noise mitigation purpose generally possess numerous pores, damping sound energy through interactions of their solid skeletons and the wave driven air. Currently prevalent sound absorbing materials (SAMs) include open cell foams,<sup>1-3</sup> fibers or wools,<sup>4-6</sup> as well as perforated panels<sup>7</sup> or membrane structures<sup>8</sup> containing porous liners. The massive amount of intricate and interlocked irregular micropores inside these conventional SAMs are basically dimension-uncontrollable and far from optimization. Previous studies confirmed that both too big and too small pores are unfavorable to the efficiency of sound absorption. Thanks to the daily improvement of micro/nano technology, materials comprised of well-defined and regular microlattice structures nowadays can be fabricated.<sup>9</sup> Besides its prominent performance in wave interference, microlattice materials are also prospective candidates for sound damping because of their porous nature. Significantly different from conventional SAMs, the microlattice material can be accurately constructed with both dimensions and locations of the pores strictly controlled, making it possible to desirably manipulate their sound damping efficiency.

A theoretical study on sound damping by SAM remains rather difficult due to the complexity of thermo-viscous acoustic wave propagation in intricate microporous structures. One popularly cited theory proposed by Biot<sup>10</sup> had to divide the problem into high and low frequency ranges in order to derive explicit solutions. Many other

---

<sup>a)</sup> Author to whom correspondence should be addressed.

theories also have to make certain assumptions to retrieve concise solutions for this complex problem.<sup>11</sup> Nevertheless, the solving approach for periodical structures like microlattice materials can be simply decomposed into the transfer matrix method (TMM).<sup>12,13</sup> However, one subtle step within TMM is the selection of impedance for “transfer matrix (TM).” Some works adopted an impedance expression from empirical approximation,<sup>12</sup> while others tried to derive a more accurate one through theoretical analysis.<sup>7,14</sup> Neither empirically nor analytically deduced impedances could give enough precision when the pores are very small and closely located, especially when the pores are irregular and the number of repeat layers is large.

In this paper, we proposed an integrated method that combines numerical simulation and analytical study to predict and optimize the sound absorption of microlattice materials. Our approach includes two steps. First, the acoustic pressure and particle velocity field of air passing one layer of the microlattice is numerically acquired, through which the effective wavenumber and impedance of this layer is calculated. Then, the retrieved effective wavenumber and impedance are used in a TM to further calculate the overall impedance of the entire microlattice material.

One illustration of microlattice material for sound absorbing is shown in Fig. 1(a). The microlattice material is backed by a rigid wall, and comprises stacks of layers in the  $X$  axis, while their patterns or features exist in the  $YZ$  plane. The microlattice material contains an  $N$ -layer of self-supportive membranes, with the thickness of each layer being  $t_n$ , the space occupied by each layer being  $a_n$ . For simplicity, we assume  $t_n = t$  and  $a_n = a$ . The success of TMM highly depends on the accuracy of the TM. In our TMM, the connection of pressures  $p$  and particle velocities  $u$  [shown in Fig. 1(c)] between two adjacent layers is established by a TM  $[T_n]$  according to  $[p_n \ u_n]^T = [p_{n+1} \ u_{n+1}]^T [T_n]$ , in which the position of  $p_n$  and  $u_n$  is selected in the center of two adjacent layers [indicated by  $\sigma$  and  $\delta$ , different from  $\phi$  and  $\varphi$  as used in classic TMM, as shown in Fig. 1(b)]. When sound waves propagate in the microlattice, the thermo-viscous effect has to be considered for solving the acoustic wave damping problem, due to the viscosity of air in tiny structures. This thermo-viscous effect on the sound wave can be characterized by using a complex wave number  $k_{\text{eff},n}$  and characteristic impedance  $Z_{\text{eff},n}$ . So a general expression is adopted as follows:

$$[T_n] = \begin{bmatrix} \cos(k_{\text{eff},n}a) & jZ_{\text{eff},n} \sin(k_{\text{eff},n}a) \\ j \sin(k_{\text{eff},n}a)/Z_{\text{eff},n} & \cos(k_{\text{eff},n}a) \end{bmatrix}. \quad (1)$$

The TM  $[T_n]$  can be solved by using Comsol Multiphysics. As shown in Fig. 1(b), a representative element of air medium extracted from the microlattice is assigned as the thermoacoustic model, while solid structures of the microlattice are realized by using “sound hard walls.” Periodic boundary conditions are applied to all four sides of the element. Taking the  $n$ th layer out of the microlattice system independently, and applying sinusoidal pressurized thermo-viscous air flow normally, the pressures ( $p_\sigma, p_\delta$ ) and

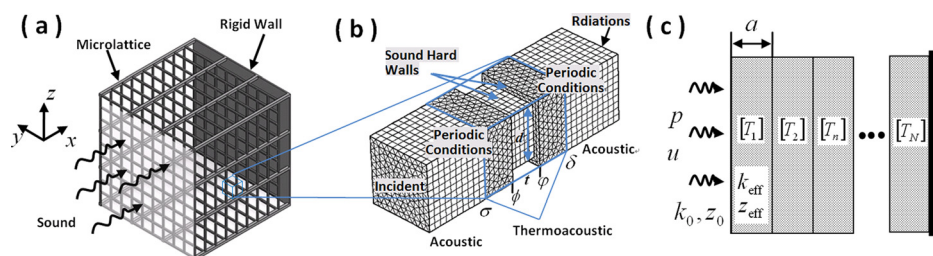


Fig. 1. (Color online) Schematic of SAMs comprised of microlattice, with (a) illustrating sound wave impinging onto a microlattice backed by rigid wall, (b) cross sectional view of the model, and (c) illustrating the integrated TMM.

flow velocities ( $u_\sigma, u_\delta$ ) at each side of the layer can be numerically calculated, and their relations can also be established through  $[T_n]$  as  $[p_\sigma \ u_\sigma] = [p_\delta \ u_\delta][T_n]^T$ .

With pressures ( $p_\sigma, p_\delta$ ) and flow velocities ( $u_\sigma, u_\delta$ ) being obtained from simulation, the characteristic impedance  $Z_{\text{eff},n}$  and other variables  $[\cos(k_{\text{eff},n}a), \sin(k_{\text{eff},n}a)]$  can be written in the form of  $p_\sigma, u_\sigma, p_\delta$ , and  $u_\delta$  as follows, and finally we have

$$[T_n] = \begin{bmatrix} t_1/t_2 & Z_{\text{eff},n}^2 t_3/t_4 \\ t_3/t_4 & t_1/t_2 \end{bmatrix}, \quad (2)$$

where  $t_1 = u_\delta p_\delta + u_\sigma p_\sigma$ ,  $t_2 = u_\delta p_\sigma + u_\sigma p_\delta$ ,  $t_3 = u_\delta p_\sigma - u_\sigma p_\delta$ ,  $t_4 = -p_\delta^2 + u_\delta^2 Z_{\text{eff},n}^2$ , and  $Z_{\text{eff},n}^2 = (p_\sigma^2 - p_\delta^2)/(u_\sigma^2 - u_\delta^2)$ . The TMs for every other layer can be determined in a similar way. For microlattice comprising multiply same layers, the overall TM can be found just by repeatedly using the TM of the  $n$ th layer. So the overall TM can be assembled as:  $[\mathbf{T}] = [T_1][T_2] \cdots [T_n] \cdots [T_N]$ . Once the overall TM is derived, the sound absorption coefficient can be readily found by using the standard deduction procedure, which would yield  $\alpha = 1 - |r|^2$ , with  $r = (T_{11} - Z_0 T_{21})/(T_{11} + Z_0 T_{21})$ , where  $Z_0$  is the characteristic impedance of air, and  $T_{11}$  and  $T_{21}$  are the components of  $[\mathbf{T}]$ .

## 2. Verification and comparison

To validate the proposed integrated TMM and compare it with the traditional TMM in terms of accuracy, sound absorption coefficients of microlattices with various structural parameters have been calculated. In calculation, all these microlattice materials are placed before a rigid wall with certain distance, indicated by “Gap  $D$ .” Most of the parameters are selected to meet the preconditions for which conventional TMMs are effective, i.e., low porosity ( $<10\%$ ), thin layer ( $\leq 0.1$  mm) between each layers. For the conventional TMM, its impedance function is chosen from the most frequently cited work of Maa.<sup>7</sup>

Figure 2(a) shows the predictions of sound absorption by one layer of a perforated panel (Fig. 4 in Ref. 13) according to the conventional TMM and integrated TMM, respectively. Since the structural parameters all satisfy the requirement of a conventional TMM, both of the predictions agree well with each other and match the measurement. However, the capability of a conventional TMM will be remarkably weakened when the structural parameters of microlattice materials no longer meet those requirements. Figure 2(b) shows the absorption coefficient of a microlattice material composed of alternatively overlapped strips. Each circular layer has parallel strips fabricated by a cutting plotter, and crossly overlaps with a neighboring layer to form square pores. In total, 44 layers are stacked together, forming 22 layers of pores. Disk shaped samples are prepared and mounted in an acoustic impedance tube (BSWA Tech, Beijing, 260) for a sound absorbing coefficient measurement, according to ISO standard procedures.<sup>15</sup> The integrated TMM provides an absorption curve that matches the measured results at most frequencies. A slightly poor prediction only exists at high frequencies, for which sound wave is more sensitive to the irregularity of the pores induced by the deformation of the thin stripes. However, the conventional TMM

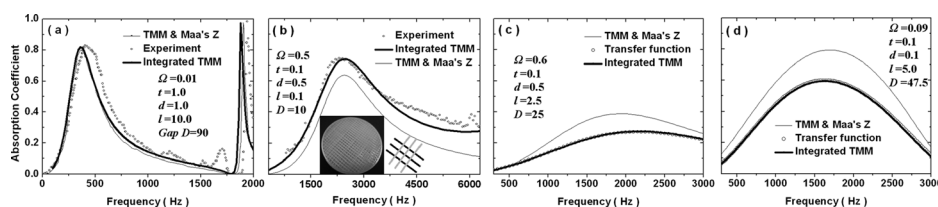


Fig. 2. Comparison of predicted sound absorbing coefficients between a conventional TMM and the integrated TMM for (a) a perforated panel with large pores, low porosity, small thickness and big spacing, (b) a crossly overlapped strip with high porosity and small spacing, (c) microlattice materials having high porosity, and (d) microlattice materials having high porosity, large layer thickness.

presents a prediction generally much lower than experimental results. It is because this microlattice material has a high porosity of 50% and very close spacing. The interactions from neighboring pores and layers greatly weaken the basis of Maa's theory on the impedance of the pores.

By keeping other parameters in favor of conventional TMMs but using a high porosity, Fig. 2(c) shows the absorption coefficient of a microlattice with high porosity (60%). A reference result indicated by circles is retrieved from the transfer function method,<sup>15</sup> which is a widely used approach for determining a material's sound absorption coefficient from acoustic pressure measurement. As revealed by Fig. 2(c), a very good match exists between our integrated TMM and transfer function method. In great contrast, the conventional TMM introduces an obvious error because of the high porosity. Since the conventional TMM calculates the impedance from a single pore independently, it produces larger impedance for a plate containing a huge number of closely placed pores. Accordingly, the predicted sound absorption is higher than the real situation. Figure 2(d) shows the absorption performance of a thin plate with very small pores ( $d=0.1$  mm). The results derived from integrated TMMs agree well with that from the transfer function method. A classic TMM gives a higher evaluation on the absorption for small pores. In Maa's work, he mentioned that the impedance of a porous plate obtained by previous works was too high,<sup>7</sup> so he suggested an equation in which the impedance was inversely related to the sectional area of the pores [Eq. (5) in Ref. 7]. When the pore diameter reduces to sub-millimeter, his estimation may still be slightly higher than that in a real situation, as can be seen from the results in Fig. 2(d).

### 3. Optimization on pore size and porosity

For a porous SAM placed in front of a rigid wall, the input impedance of the bulk material is determined by both the characteristic impedance  $Z_{\text{eff}}$  and the wave number  $k_{\text{eff}}$  of the microlattice materials:  $Z_{\text{in}} = -iZ_{\text{eff}}\cot(k_{\text{eff}}L)$ ,<sup>16</sup> with  $L$  being the total length of the SAM. To ensure the impedance match, we have  $Z_0 = -iZ_{\text{eff}}\cot(k_{\text{eff}}L)$ , which yields  $Z_{\text{eff}}/Z_0 = i\tan(k_{\text{eff}}L)$ , representing the requirement of a positive relation of the characteristic impedance  $Z_{\text{eff}}$  and the wave number  $k_{\text{eff}}$ . However,  $Z_{\text{eff}}$  and  $k_{\text{eff}}$  are actually inversely related in a porous material. As can be found in Ref. 16, for a material formed by parallel straight tubes, the proximate relation of impedance and wave number can be expressed by:  $Z_{\text{eff}}/Z_0 \propto G \propto 1/\Gamma \propto 1/k_{\text{eff}}$ , where  $G$  and  $\Gamma$  are two correction coefficients for impedance and wave number, respectively, both of which were tightly determined by the pore size and porosity. So, if  $Z_{\text{eff}}$  is too large, the incident sound wave will be reflected by the SAM directly, without even meeting the back wall. On the other hand, if  $Z_{\text{eff}}$  is too small, the SAM would not be dissipative enough, causing sound wave reflected by the back wall. Therefore, there exists an optimized pore size and porosity enabling the SAM to be most efficient.

The optimization will be conducted on microlattices to determine the best pore size and porosity that result in a target sound absorption over a frequency band. The target sound absorption will be described by using the Sound Absorption Average (SAA) as suggested by ASTM-C423.<sup>17</sup> SAA is the average of the absorption coefficients at twelve 1/3 octave frequency bands from 200 to 2500 Hz. The porosity of the pores under study is set between 0.09 and 0.7 and the size ranges between 0.15 and 0.25 mm, with pores assumed to be square. For each combination of the pore size and porosity, the transfer matrices of the microlattice at twelve 1/3 octave frequencies are calculated. Accordingly, the sound absorption coefficients at those frequencies for different overall lengths (50 mm, 40 mm) have been calculated. After that, the SAA at each combination of pore size and porosity is found. The results for pore size above 0.25 are shown in Fig. 3.

As it appears in Figs. 3(a) and 3(b), an overall thickness of 50 mm generates a maximum SAA as high as 0.75, with the peak SAA occurring when the pore size is around 0.2 mm and porosity 0.4. Similarly, when the overall thickness is reduced to 40 mm, a peak SAA also appears at a pore size of 0.2 mm, while generally the SAA is

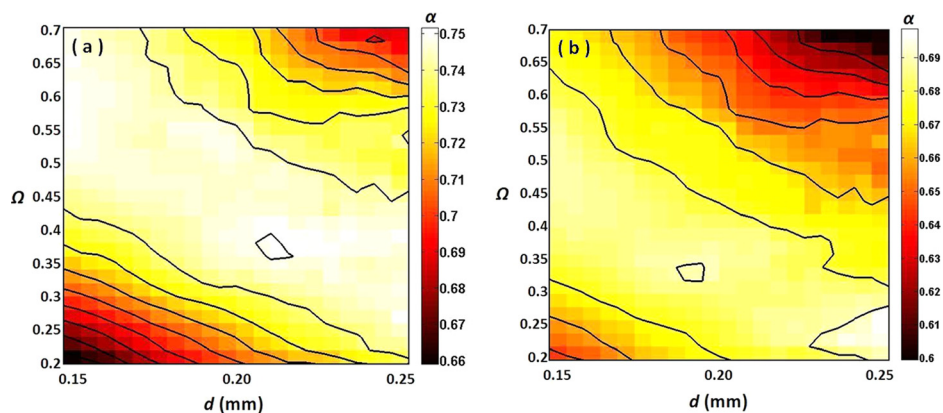


Fig. 3. (Color online) SAA of microlattice materials of various combinations of pore sizes (0.15–0.25 mm) and porosities (0.2–0.7) at overall thickness of (a) 50 mm and (b) 40 mm.

lower than that of 50 mm. As it is revealed, an approximate condition for achieving maximum SAA would be  $\Omega = -2d + 0.85$ , where  $d$  is specified in millimeters, and  $\Omega$  is dimensionless. This can be interpreted as larger pores having small flow impedances, making the structure less dispersive; thus increasing the wave path is a necessary way to improve the sound absorption. If the pore size is too large, it is almost impossible to generate a large SAA within a reasonable thickness.

As can be noted in Fig. 3, the thickness of the SAM plays a subtle role in sound absorbing coefficient, and usually when the porosity is high, a thicker SAM performs better. In real applications, people prefer the SAM having a smaller overall thickness. Therefore, the overall thickness is chosen as the reference criteria for optimization. If the target SAA is set at a certain value, say, 0.7, then the goal of the optimization is to determine what pore size and porosity requires the smallest thickness to make the SAA reach 0.7. Considering the fabrication precision of the current three-dimensional (3D) printer, the porosity is selected between 0.3 and 0.7. Figure 4 shows the obtained results of required thickness for pore size between 0.15 and 0.5 mm. Obviously, pore size under 0.25 mm is advantageous for sound absorption, a smaller overall thickness is required to attain a target SAA. A similar situation can also be found when SAAs are set at other values. Minimum thickness appears when the pore

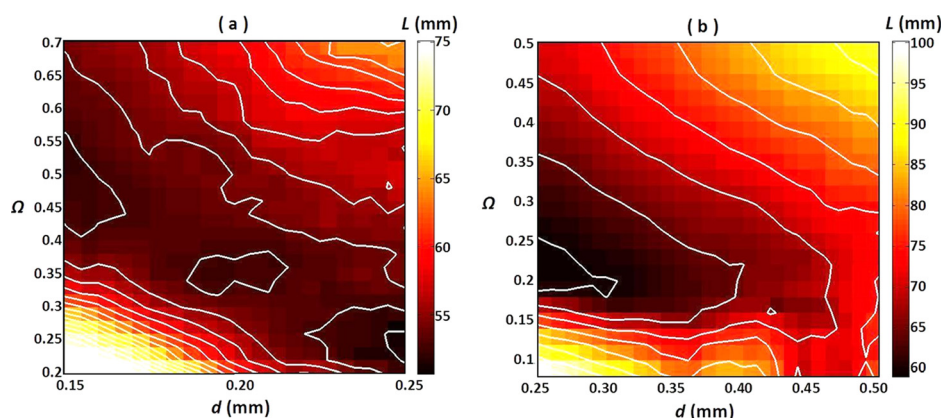


Fig. 4. (Color online) To achieve a target SAA (0.7), the required thickness for microlattice materials comprised of various pores and porosities, with combinations of (a) pore sizes between 0.15 and 0.25 mm, porosities between 0.2 and 0.7; (b) pore sizes between 0.25 and 0.5 mm, porosities between 0.09 and 0.5.

size is around 0.2 mm. The above mentioned relation of pore size and porosity  $\Omega = -2d + 0.85$  is also applicable to this case.

#### 4. Conclusion

To characterize the absorbing efficacy of the microlattice materials, an integrated TMM has been proposed. By comparing with a conventional TMM, the proposed integrated TMM gives better prediction of sound absorption by microlattice materials. This verifies the validity of the proposed integrated TMM and shows its advantage over a conventional TMM. Generally, when the pores are small and porosity is high, the integrated TMM introduces lower errors as compared with a conventional TMM. Finally, the integrated TMM is adopted to optimize the pore size and porosity of the microlattice materials. A pore size of 0.2 mm is found to be optimal for a microlattice material to attain a target SAA with the smallest thickness.

#### Acknowledgment

This work was supported by Natural Science and Engineering Research Council of Canada (NSERC) and Research Accelerator Grant of The University of Western Ontario.

#### References and links

- <sup>1</sup>X. Wang and T. J. Lu, "Optimized acoustic properties of cellular solids," *J. Acoust. Soc. Am.* **106**, 756–765 (1999).
- <sup>2</sup>F. Han, G. Seiffert, Y. Zhao, and B. Gibbs, "Acoustic absorption behaviour of an open-celled aluminium foam," *J. Phys. D: Appl. Phys.* **36**, 294–302 (2003).
- <sup>3</sup>M. Hakamada, T. Kuromura, Y. Chen, H. Kusuda, and M. Mabuchi, "High sound absorption of porous aluminum fabricated by spacer method," *Appl. Phys. Lett.* **88**, 254106 (2006).
- <sup>4</sup>N. Atalla, R. Panneton, F. C. Sgard, and X. Olny, "Acoustic absorption of macro-perforated porous materials," *J. Sound Vib.* **243**, 659–678 (2001).
- <sup>5</sup>J. P. Arenas and M. J. Crocker, "Recent trends in porous sound-absorbing materials," *Sound Vib.* **44**, 12–17 (2010).
- <sup>6</sup>J. Mohrova and K. Kalinova, "Different structures of PVA nanofibrous membrane for sound absorption application," *J. Nanomater.* **2012**, 1–4.
- <sup>7</sup>D. Maa, "Potential of microperforated panel absorber," *J. Acoust. Soc. Am.* **104**, 2861–2866 (1998).
- <sup>8</sup>J. Mei, G. Ma, M. Yang, Z. Yang, W. Wen, and P. Sheng, "Dark acoustic metamaterials as super absorbers for low-frequency sound," *Nat. Commun.* **3**, 756 (2012).
- <sup>9</sup>T. A. Schaedler, A. J. Jacobsen, A. Torrents, A. E. Sorensen, J. Lian, J. R. Greer, L. Valdevit, and W. B. Carter, "Ultralight metallic microlattices," *Science* **334**, 962–965 (2011).
- <sup>10</sup>M. A. Biot, "Theory of propagation of elastic waves in a fluid-saturated porous solid. I. Low-frequency range," *J. Acoust. Soc. Am.* **28**, 168–178 (1956).
- <sup>11</sup>E. Blanc, G. Chiavassa, and B. Lombard, "Time-domain numerical modeling of two-dimensional wave propagation in porous media with frequency-dependent dynamic permeability," *J. Acoust. Soc. Am.* **134**, 4610–4623 (2013).
- <sup>12</sup>D. H. Lee and Y. P. Kwon, "Estimation of the absorption performance of multiple layer perforated panel systems by transfer matrix method," *J. Sound Vib.* **278**, 847–860 (2004).
- <sup>13</sup>Z. Tao, B. Zhang, D. W. Herrin, and A. F. Seybert, "Prediction of sound-absorbing performance of micro-perforated panels using the transfer matrix method," *2005 SAE Noise and Vibration Conference Proceedings*, Traverse City, MI, 2005.
- <sup>14</sup>M. R. Stinson, "The propagation of plane sound waves in narrow and wide circular tubes, and generalization to uniform tubes of arbitrary cross-sectional shape," *J. Acoust. Soc. Am.* **89**, 550–558 (1991).
- <sup>15</sup>ISO 10534-2, *Acoustics—Determination of sound absorption coefficient and impedance in impedance tubes—Part 2: Transfer-function method*, 1st ed. (BSI Group, London, 1998).
- <sup>16</sup>J. F. Allard and N. Atalla, *Propagation of Sound in Porous Media: Modeling Sound Absorbing Materials*, 2nd ed. (Elsevier Applied Science, New York, 2009).
- <sup>17</sup>ASTM C423-09a, *Standard Test Method for Sound Absorption and Sound Absorption Coefficients by the Reverberation Room Method* (ASTM, West Conshohocken, PA, 2009).